Twin axial vortices generated by Fibonacci lenses

Arnau Calatayud,[1] **Vicente Ferrando,**[1,2] **Laura Remón,**[1]
Walter D. Furlan,[2] **and Juan A. Monsoriu**[1,*]

[1]*Centro de Tecnologías Físicas, Universitat Politècnica de València, 46022 Valencia, Spain*
[2]*Departamento de Óptica, Universitat de València, 46100 Burjassot, Spain*

**jmonsori@fis.upv.es*

Abstract: Optical vortex beams, generated by Diffractive Optical Elements (DOEs), are capable of creating optical traps and other multi-functional micromanipulators for very specific tasks in the microscopic scale. Using the Fibonacci sequence, we have discovered a new family of DOEs that inherently behave as bifocal vortex lenses, and where the ratio of the two focal distances approaches the golden mean. The disctintive optical properties of these Fibonacci vortex lenses are experimentally demonstrated. We believe that the versatility and potential scalability of these lenses may allow for new applications in micro and nanophotonics.

OCIS codes: (050.1940) Diffraction, (050.1970) Diffractive Optics, (050.4865) Optical Vortices.

References and links

1. A. Sakdinawat and Y. Liu, "Soft-x-ray microscopy using spiral zone plates," Opt. Lett. **32**, 2635–2637 (2007).
2. A. A. Siemion, M. Makowski, J. Suszek, J. Bomba, A. Czerwinski, F. Garet, J.-L. Coutaz, and M. Sypek, "Diffractive paper lens for terahertz optics," Opt. Lett. **37**, 4320–4322 (2012).
3. G. Saavedra, W. D. Furlan, and J. A. Monsoriu, "Fractal zone plates," Opt. Lett. **28**, 971–973 (2003).
4. J. A. Davis, S. P. Sigarlaki, J. M. Craven, and M. L. Calvo, "Fourier series analysis of fractal lenses: theory and experiments with a liquid-crystal display," Appl. Opt. **45**, 1187 (2006).
5. W. D. Furlan, G. Saavedra, and J. A. Monsoriu, "White-light imaging with fractal zone plates," Opt. Lett. **32**, 2109–2111 (2007).
6. F. S. Roux, "Distribution of angular momentum and vortex morphology in optical beams," Opt. Commun. **242**, 45–55 (2004).
7. G. Gbur and T. D. Visser, "Phase singularities and coherence vortices in linear optical systems," Opt. Commun. **259**, 428–435 (2006).
8. A. Bishop, T. Nieminen, N. Heckenberg, and H. Rubinsztein-Dunlop, "Optical application and measurement of torque on microparticles of isotropic nonabsorbing material," Phys. Rev. A **68**, 033802 (2003).
9. K. Ladavac and D. G. Grier, "Microoptomechanical pumps assembled and driven by holographic optical vortex arrays," Opt. Express **12**, 1144 (2004), http://www.opticsexpress.org/abstract.cfm?URI=oe-12-6-1144.
10. W. M. Lee, X.-C. Yuan, and W. C. Cheong, "Optical vortex beam shaping by use of highly efficient irregular spiral phase plates for optical micromanipulation," Opt. Lett. **29**, 1796 (2004).
11. S. H. Tao, X.-C. Yuan, J. Lin, and R. E. Burge, "Sequence of focused optical vortices generated by a spiral fractal zone plate," Appl. Phys. Lett. **89**, 031105 (2006).
12. W. D. Furlan, F. Giménez, A. Calatayud, and J. A. Monsoriu, "Devils vortex-lenses," Opt. Express **17**, 21891 (2009), http://www.opticsexpress.org/abstract.cfm?URI=oe-17-24-21891.
13. J. A. Monsoriu, A. Calatayud, L. Remón, W. D. Furlan, G. Saavedra, and P. Andrés, "Zone plates generated with the Fibonacci sequence," in *Proceedings of EOS Topical Meeting on Diffractive Optics*, pp. 151–152 (2010).
14. J. A. Monsoriu, A. Calatayud, L. Remón, W. D. Furlan, G. Saavedra, and P. Andrés,"Bifocal Fibonacci diffractive lenses," IEEE Photon. J. (to be published), DOI: 10.1109/JPHOT.2013.2248707.
15. E. Maciá, "Exploiting aperiodic designs in nanophotonic devices," Rep. Prog. Phys. **75**, 1–42 (2012).
16. Y. Sah and G. Ranganath, "Optical diffraction in some Fibonacci structures," Opt. Commun. **114**, 18–24 (1995).

17. N. Gao, Y. Zhang, and C. Xie, "Circular Fibonacci gratings," Appl. Opt. **50**, G142–G148 (2011).
18. H. T. Dai, Y. J. Liu, and X. W. Sun, "The focusing property of the spiral Fibonacci zone plate," in *Optical Components and Materials IX*, S. Jiang, M. J. F. Digonnet, and J. C. Dries, eds., Proc. SPIE **8257**, 82570T1 (2012).
19. J. Swartzlander, "Peering into darkness with a vortex spatial filter," Opt. Lett. **26**, 497 (2001).
20. J. E. Curtis and D. G. Grier, "Structure of optical vortices," Phys. Rev. Lett. **90**, 133901 (2003).
21. A. Calatayud, W. D. Furlan, and J. A. Monsoriu, "Experimental generation and characterization of devils vortex-lenses," Appl. Phys. B **106**, 915–919 (2012).

1. Introduction

In photonics technology, Diffrative Optical Elements (DOEs) have found a large number of new aplications in many different areas, covering the whole electromagnetic spectrum from X-ray Microscopy [1], to THz Imaging [2]. Difractive lenses such as conventional Fresnel zone plates, are essential in many focusing and image forming systems but they have inherent limitations. Fractal zone plates are a new type of multifocal diffractive lenses that have been proposed to overcome some of these limitations, mainly under polychromatic illumination [3, 4]. In fact, it was shown that these lenses, generated with the fractal Cantor set have an improved behavior, especially under wide band illumination [5].

DOEs have been also designed to generate optical vortices. Optical vortices are high value optical traps because in addition to trap microparticles they are capable to set these particles into rotation due to its inherent orbital angular moment [6, 7]. These special optical beams have been used, for exemple, as actuators and testers in micromechanical systems [8]. Arrays of optical vortices have shown the ability to assemble and drive mesoscopic optical pumps in microfluidic systems [9].

Among the several methods that have been proposed for optical vortices generation, spiral phase plates [10] stands out, mainly because they provide high energy efficiency. Spiral phase plates have been recently combined with Fractal Zone Plates to produce a sequence of focused optical vortices along the propagation direction [11, 12].

In this work we present the Fibonacci Vortex Lenses (FVLs), which are able to generate simultaneously two optical vortices along the axial coordinate whose diametres are related by the golden mean. These new type of DOEs are constructed using the Fibonacci sequence [13, 14] along the squared radial coordinate. This sequence has been also employed in the development of different photonic devices [15], such as multilayers and linear gratings [16], circular gratings [17], spiral zone plates [18].

2. Fibonacci vortex lenses design

A FVL is defined as a pure phase diffractive element whose phase distribution is given by $\Phi_{FVL}(\zeta,\theta_0) = mod_{2\pi}[\Phi_a(\theta_0)+\Phi_j(\zeta)]$. It combines the azimuthal phase variation that characerizes a vortex lens, i.e. $\Phi_a = m\theta_0$, where m is a non zero integer called the topological charge [18] and θ_0 is the azimuthal angle about the optical axis at the pupil plane, with the radial phase distribution that is generated through the Fibonacci sequence in the following way:

Starting with two elements (seeds) $F_0 = 0$ and $F_1 = 1$, the Fibonacci numbers, $F_j = \{0,1,1,2,3,\ 5,8,13,21,\ldots\}$, are obtained by the sequential application of the following rule: $F_{j+1} = F_j + F_{j-1}$, $(j = 0,1,2,\ldots)$. The golden mean, or golden ratio, is defined as the limit of the ratio of two consecutive Fibonacci numbers:

$$\varphi = \lim_{j\to\infty} F_j/F_{j-1} = \left(1+\sqrt{5}\right)/2\,. \tag{1}$$

Based on the Fibonacci numbers, a binary aperiodic Fibonacci sequence can also be generated with two seed elements, as for exemple, $S_1 = \{A\}$ and $S_0 = \{B\}$. Then, next order of the

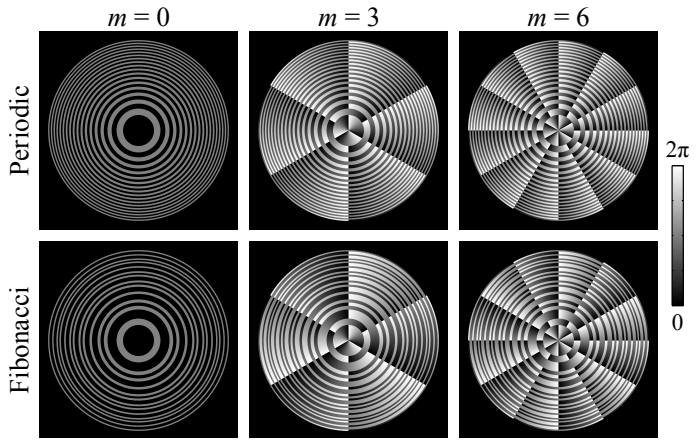

Fig. 1. Bottom: Phase distributions of FVLs based on the Fibonacci sequence S_8, with different topological charges. Top: The equivalent periodic lenses with the same number of zones.

sequence is obtained simply as the concatenation of the two previous ones: $S_{j+1} = \{S_j S_{j-1}\}$ for $j \geq 1$. Therefore, $S_2 = \{AB\}$, $S_3 = \{ABA\}$, $S_4 = \{ABAAB\}$, $S_5 = \{ABAABABA\}$, etc. Note that, in each sequence, two succesive "B" are separated by either, one or two "A", and that the total number of elements of the order j sequence is F_{j+1}, which results from the sum of F_j elements "A", plus F_{j-1} elements "B". Each of these sequences can be used to define the binary generating function for the radial phase distribution of the FVL. For our purpose, the generating function, $\Phi_j(\zeta)$, is defined in the domain $[0,1]$, and this interval is partitioned in F_{j+1} sub-intervals of length $d = 1/F_{j+1}$. Then, the value that the function $\Phi_j(\zeta)$ takes at the k^{th} sub-interval will be 0 or π if the value of the k^{th} element of the S_j sequence, S_{jk}, is "A" or "B", respectively. Next, from a particular generating function $\Phi_j(\zeta)$, the radial part of the transmitance of the corresponding binary pure-phase FVL is obtained as $q(\zeta) = \exp[i\Phi_j(\zeta)]$, after performing the following coordinate transformation: $\zeta = (r/a)^2$, being r the radial coordinate of the lens, and a its maximum value. Typical examples of FVLs are shown in Fig. 1. For comparison, a conventional vortex lenses based on Fresnel zone plates are represented in the same figure. The corresponding Fresnel zone plates can be considered periodic structures along the square radial coordinate ζ having the same number of elements, F_{j+1}, with period $p = 2d$, but where the position of some zones with different phase have been interchanged. Moreover, taking into account that Fibonacci sequences are aperiodic, but with two inconmmensurable periods [15], is easy to show that, according to our nomenclature, in a FL these periods are related to the period of the equivalent zone plate through $p_1 = 1/F_{j-1} \approx 0.5\,(\varphi+1)\,p$; and $p_2 = 1/F_j \approx 0.5\,\varphi\,p$. Thus, a FL can be understood as two Fresnel zone plates interlaced.

3. Focusing properties

To study the focusing properties of FVLs we have computed the irradiance provided by the transmitance of this lens, $t(\zeta,\theta_0) = q(\zeta)\exp[im\theta_0]$, when it is illuminated by a plane wave of wavelength λ. Within the Fresnel approximation the irradiance function is given by:

$$I(u,v,\theta) = u^2 \left| \int_0^1 \int_0^{2\pi} t(\zeta,\theta_0) \exp\left(-i2\pi u\zeta\right) \exp\left[i4\pi uv\zeta^{1/2}\cos\left(\theta-\theta_0\right)\right] d\zeta\, d\theta_0 \right|^2 , \quad (2)$$

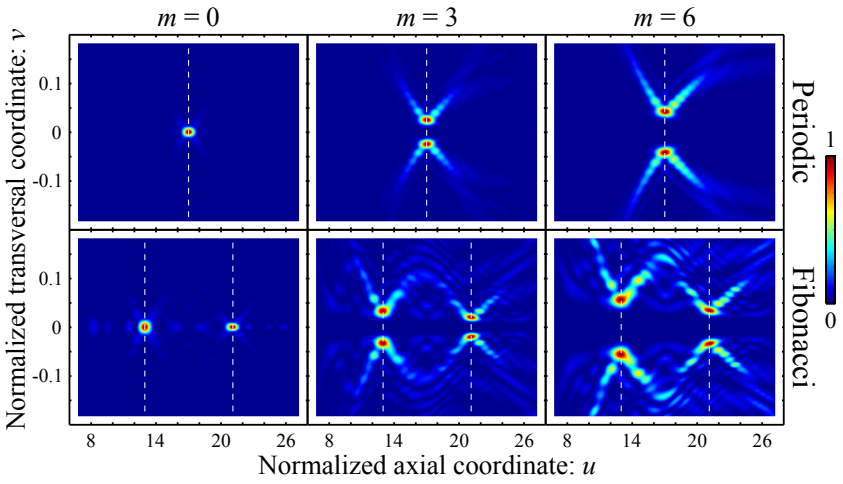

Fig. 2. Evolution of the transverse irradiance for S_8 based FVLs with different topological charges and their periodic equivalent lenses.

where $u = a^2/2\lambda z$ is the normalized axial coordinate and $v = r/a$ is the normalized transverse coordinate. Replacing $t(\zeta,\theta_0)$ and taking into account that

$$\int_0^{2\pi} \exp(im\theta_0)\exp\left[i4\pi uv\zeta^{1/2}\cos(\theta-\theta_0)\right]d\theta_0 = 2\pi\exp\left[im\left(\theta+\frac{\pi}{2}\right)\right]J_m\left(4\pi uv\zeta^{1/2}\right), \tag{3}$$

Eq. (2) is reduced to

$$I(u,v) = 4\pi^2u^2\left|\int_0^1 q(\zeta)\exp(-i2\pi u\zeta)\,J_m\left(4\pi uv\zeta^{1/2}\right)d\zeta\right|^2, \tag{4}$$

being $J_m()$ the Bessel function of the first kind of order m.

By using Eq. (4) we have computed the irradiances provided by the lenses shown in Fig. 1. The integrals were numerically evaluated applying the Simpson's rule using a step length $1/2000$. The result is shown in Fig. 2. It can be seen that FVLs produce a twin foci whose positions are given by the Fibonacci numbers. In this case, for S_8 FVLs, the first focus is located at $u_1 = 13 = F_{j-1} = 1/p_1$ and the other one at $u_2 = 21 = F_j = 1/p_2$. Thus, the ratio of the focal distances satisfies $u_2/u_1 \approx \varphi$. Note also that, for non-null values of the topological charge, each focus is a vortex, thus, in general, a pair of doughnut shaped foci is generated by a FVL. Comparing the diffraction patterns provided by FVLs with different topological charges it can be verified that the diameter of the doughnuts increases with the topological charge as those produced by conventional vortex lenses [19, 20].

4. Experimental results

For the experimental study of the properties of FVLs, we implemented the experimental setup shown in Fig 3. The proposed lenses were recorded on a Liquid Crystal in a Silicon SLM (Holoeye PLUTO, 8-bit gray-level, pixel size $8\,\mu$m and resolution equal to 1920×1080 pixels), calibrated for a 2π phase shift at $\lambda = 633$nm operating in phase-only modulation mode. The procedure to compensate the wavefront distorsions caused by the lack of flatness of the SLM and the other optical components was detailed elsewhere [21]. In addition to the diffractive lenses, a linear phase carrier was modulated on the SLM to avoid the noise originated by

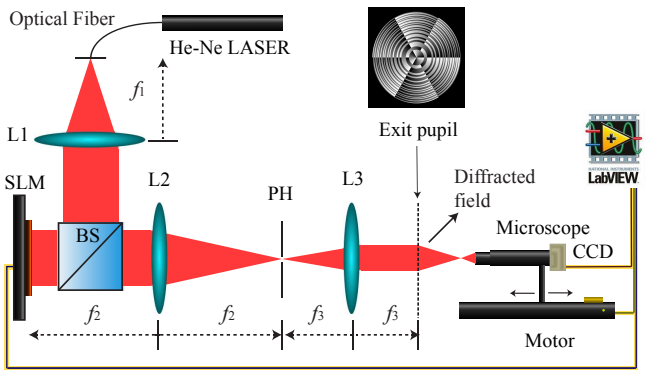

Fig. 3. Experimental setup used for studying the focusing properties of FVLs.

the specular reflection (zero order diffraction) and the pixelated structure of the SLM (higher diffraction orders). This linear phase is compensated by tilting the SLM and a pin-hole (PH) is used to filter all diffraction orders except the first one. Then at the L3 lens focal plane (exit pupil) a rescaled image of the desired lens pupil is achieved. A collimated beam (He-Ne Laser $\lambda = 633\,\text{nm}$) impinges onto the SLM and the diffracted field is captured and registered with a microscope (4x Zeiss Plan-Apochromat objective) attached to a CCD camera (EO-1312M 1/2" CCD Monochrome USB Camera, 8-bit gray-level, pixel pitch of $4.65\,\mu\text{m}$ and 1280×1024 pixels). The microscope and the CCD are mounted on a translation stage (Thorlabs LTS 300, Range: 300 mm and $5\,\mu\text{m}$ precision) along the optical axis.

The experimental and computed irradiances produced by a S_8 FVL with topological charge $m = 6$ along the optical axis are shown in Fig. 4. Note that the vortex planes correspond to $f_1 = a^2/2\lambda F_7 \approx 7.35\,\text{cm}$ and $f_2 = a^2/2\lambda F_8 \approx 4.55\,\text{cm}$. As predicted by the theoretical analysis, the axial localization of the focal rings depends on the Fibonacci numbers F_j and F_{j-1}, and such focal distances satisfy the following relationship: $f_1/f_2 = F_j/F_{j-1} \approx \varphi$.

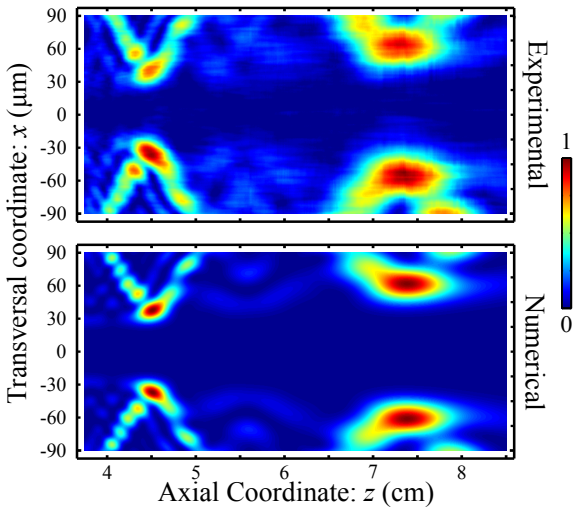

Fig. 4. Experimental and computed transverse irradiance evolution along the optical axis provided by the S_8 FVL with $m = 6$ and $a = 1.1\,\text{mm}$.

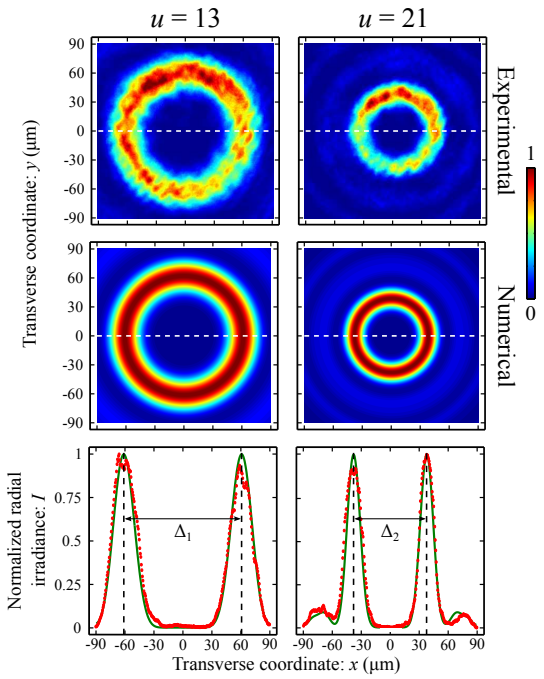

Fig. 5. Experimental and numerical transverse irradiance at the focal planes provided by the S_8 based on FVL with $m = 6$ and $a = 1.1\,\text{mm}$. The intensity profiles along the white, dotted lines are plotted (bottom) together with the numerical results for comparison.

Figure 5 shows the experimental and the numerically simulated transverse irradiance at the focal planes for the same FVL. Interestingly, the diameter of the focal rings, Δ, which also depends on the topological charge of the FVL, satisfies a similar rule i.e. $\Delta_1/\Delta_2 \approx \varphi$ (see Fig. 5). Thus, FVLs are capable of generating twin axial vortices with different, but perfectly established, diameter of the central core.

5. Conclusions

Sumarizing, a new type of bifocal vortex lenses has been introduced, whose design is based on the Fiboonacci sequence. It was found that a FVL produces a twin optical vortices along the axial coordinate. The positions of both foci depend on the two incommensurable periods of the Fibonacci sequence in which the FVL is based on. The radii of these twin vortices increase with the topological charge of the vortex lens, but always their ratio approaches the golden mean. The 3D distribution of the diffracted field provided by FVLs has been tested experimentally using a SLM. An excellent agreement between the experimental results and the theoretical predictions has been demonstrated.

Acknowledgements

We acknowledge the financial support from Ministerio de Economía y Competitividad (grants FIS2011-23175), Generalitat Valenciana (grant PROMETEO2009-077), and Universitat Politècnica de València (SP20120569), Spain. L.R. acknowledges a fellowship of “Fundación CajaMurcia”, Spain.